ENHANCED ELECTROCHEMICAL PERFORMANCE OF POROUS CARBON AEROGEL DERIVED FROM WASTE PAPER FOR SUPERCAPACITOR APPLICATIONS

Đến tòa soạn 06-04-2023

Hoanh Van Ngo[1], Hung Tran Nguyen[1], Hieu Trung Le[1], Thanh Huu Le[1], Hoa Thi Nguyen[1], Thien Tri Vu[1], Thinh Xuan Phung[2*]

[1]*Institute of Chemistry and Materials, 17 Hoang Sam Street; Cau Giay District, Hanoi City, Vietnam*

[2]*Deparment of Education, Academy of Military Science and Technology, 17 Hoang Sam Street; Cau Giay District, Hanoi City, Vietnam*

[*] Email: phungxuanthinh@hotmail.com

TÓM TẮT

ĐẶC TÍNH ĐIỆN HÓA CỦA VẬT LIỆU CACBON AEROGEL XỐP TỪ GIẤY THẢI ỨNG DỤNG TRONG SIÊU TỤ ĐIỆN

Vật liệu cacbon aerogel với cấu trúc xốp được chế tạo từ giấy thải bằng phương pháp cacbon hóa và hoạt hóa đơn giản và được sử dụng làm vật liệu cho điện cực siêu tụ điện. Cacbon aerogel thu được có diện tích bề mặt lớn, đạt 233,9 m2/g. Trong hệ tụ điện đối xứng hai điện cực, điện cực cacbon aerogel có điện dung riêng đạt 94 F/g và duy trì tuổi thọ phóng nạp cao với 92,5% dung lượng sau 1000 chu kỳ. Kết quả của nghiên cứu này cho thấy giấy thải có thể trở thành nguyên liệu chế tạo vật liệu tích trữ năng lượng hiệu suất cao.

Từ khóa: *Cacbon aerogel, giấy thải, đặc tính điện hóa, siêu tụ điện.*

1. INTRODUCTION

High quality energy storage materials have attracted great interests in many electronic equipment [1, 2]. Along with the dramatic development of electric industry and with the increased urgent demands of energy storage devices for environment - friendly high power energy source, supercapacitors (SCs) have been attracting more and more attention of researchers [3-6] because of its outstanding, such as high power density, superior cycle life, high charge and discharge rate [7-11]. Because of those advantages mentioned above, SCs make up many markets ranging from electronic to transportation and stationary applications. [12-14].

Carbon materials, including activated carbon, carbon fibers, carbon nanotubes, carbon aerogels, graphene and carbide-derived carbons, are widely used as active electrode materials [15]. These carbon materials have very good supercapacitor behavior. However, most of them are prepared from mineral materials and petroleum, which are expected to be depleted in the near future. The high cost of raw materials, environmental destructiveness of preparation and complicated manufacturing largely limit the further applications of most supercapacitors.

Therefore, many researches have focused on the utilization of green reproducible biomass or their derivatives to produce porous carbon materials, which are critical to the sustainable development and environmental protection [16-18].

For the structure of carbon materials, the electrochemical performance of SCs is dependent

on several parameters, such as the electric conductivity of the electrode materials, pore size and distribution, and specific surface area. The electric conductivity affects the power density that the ECs can deliver. The specific surface area and pore size affects the specific capacitance and energy density. For example, KOH-activated porous graphene exhibits a very high specific surface area (3100 m^2/g) [19]. However, the increase in specific surface area cannot always positively enhance the specific capacitance. This is because with increasing specific surface area, the pore volume of micropores increases and the size of the micropores decreases to below the size of hydrated electrolyte ions, which decreases the accessibility of pores. The ideal ECs electrode materials should have a hierarchical porous structure containing macropores (larger than 50 nm) for the ion-buffering reservoir, mesopores (2–50 nm) for ion transportation and micropores (less than 2 nm) for the enhancement of charge storage. Moreover, it is also desirable that the porous carbon structures should have multi-scale pores [20].

In this study, porous carbon aerogel was prepared from freeze-drying cellulose aerogel using recycling paper as raw material. The direct carbonization of cellulose aerogel creates numerous macro- and meso-pores following scheme in Fig. 1.

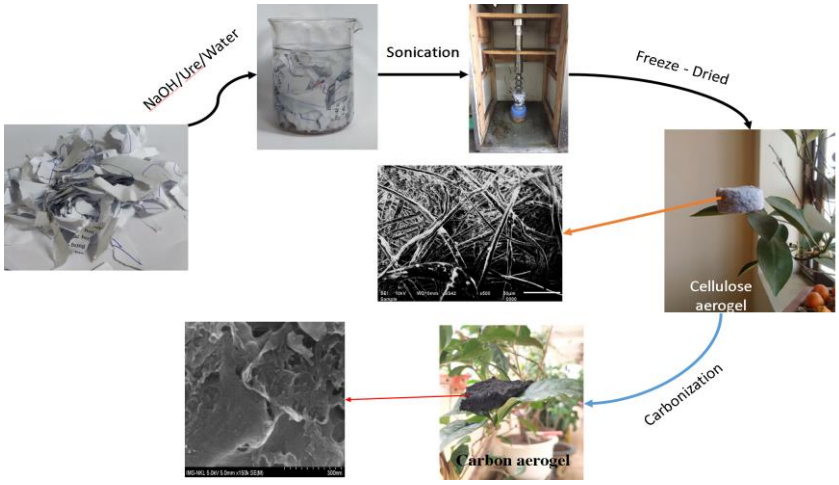

Fig 1. The synthetic scheme of carbon aerogel from waste paper

2. EXPERIMENTAL

2.1 Materials

Waste paper scraps. Other chemicals such as Urea, NaOH were reagent grade and used without further purification. De-ionized water was used throughout the experiments.

2.2 Preparation of cellulose aerogel

2 g of waste paper scraps were impregnated in 80 mL de-ionized water for 1 hour. Then, NaOH and Urea were added into the mixture. The mixture was ultrasonicated for 30 minutes. After sonication, the mixture was aged at -20 ^oC.

The wet gel was removed and placed in a plastic container, and the solvent was exchanged with ethanol 5 times and with DI water 5 times. Test the pH of the water until it reached neutral. These gel samples were aged at -50^oC for 8 h, freeze dried for 48 hours to obtain cellulose aerogel.

2.3 Preparation of carbon aerogel

The resultant cellulose aerogels were pyrolyzed at 800 ^oC (10 ^oC/min) for 90 minutes under flowing N_2 gas.

2.4 Characterizations of carbon aerogel

The morphologies and structural properties of the prepared materials were characterized by field emission scanning electron microscopy (FESEM; HITACHI S-4800). The porous characteristics of the prepared materials were examined by N_2 adsorption/desorption experiments at 77 K using ASAP 2020 V3.02 H. The specific surface area was measured according to the Brunauer-Emmett-

Teller (BET) method, and the BJH method was used to calculate the pore size distribution and pore volumes.

2.5 Electrochemical measurements

To obtain the electrochemical measurements of the prepared sample, the two-electrode configuration was used. In order to prepare the electrode, in the two-electrode set-up, according to the optimization methods, the supercapacitor electrodes were made of different activated carbon aerogels, conductive (carbon super-P), and the binder (PVDF) with weight ratio of 8:1:1. After milling by ball mill for 8 hours, the mixture was pressed onto a nickel foil with a size ϕ= 8 mm. The prepared electrodes were then dried at 80 ^{o}C in vacuum for 12 hours to remove solution. An aqueous solution of 6 M KOH was used as the electrolyte.

Two electrodes made by the method mentioned above and separator were immersed into the 6 M KOH electrolyte. Then, two electrodes were assembled in a cell-lock.

The electrochemical performances of carbon aerogel electrodes were investigated by cyclic voltammetry (CV), gavanostatic charging-discharging (GCD) and electrochemical imdependance spectroscopy (EIS) measuraments, which were carried out by Autolab PGSTAT309n (Metrohm, Switzerland).

The specific capacitance (Cs) of the electrode materials and energy density of supercapacitor (E) were calculated according to Eq.(1) [10].

$$C_s = \frac{2I \times \Delta t}{m \times \Delta V} \quad (1)$$

where I (in A), Δt (in second), ΔV (in V), and m (in mg) are current, discharging time, potential window, and the mass of the active material on electrode, respectively.

3. RESULTS AND DISCUSSION

The main process of preparing porous carbon aerogel derived from recycling paper is schematically illustrated in Fig. 1.

The first step is the hydrolysis of cellulose. This solution was sonicated for 30 minutes and then placed in refrigerated to keep it aged. After aging and dried by freeze dryer, the cellulose aerogel can be obtained. After that, the cellulose was pyrolyzed at 800°C (10°C/min) for 90 minutes under flowing N_2 gas. Successful formation of carbon aerogel was well confirmed by XRD measurement.

Fig. 2a shows XRD spectra of carbon aerogel. XRD pattern of carbon aerogel shows the major peaks at 2θ =25.6° and 43°, associated with diffraction of graphitic carbon of (002) and (101), respectively.

To examine the morphology of cellulose aerogel and carbon aerogel, all of the carbon aerogel samples examined by SEM and FESEM, and the results are demonstrated in Fig.3, which describes the general morphology of synthesized cellulose aerogel and carbon aerogel.

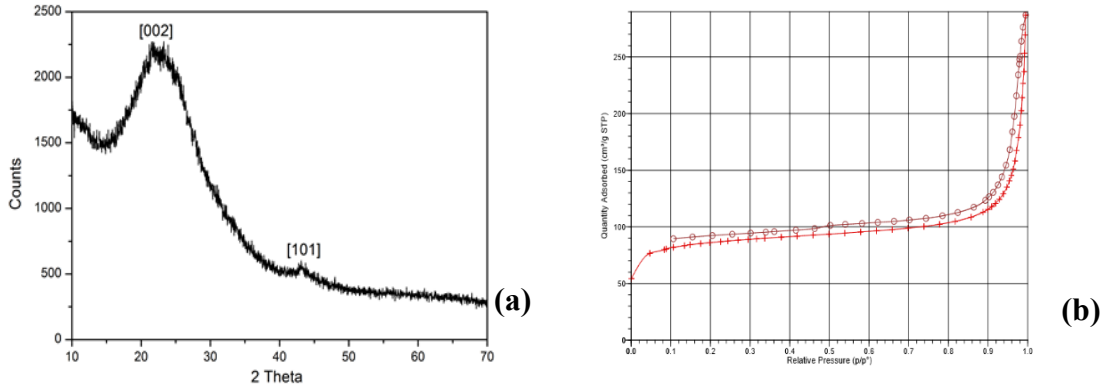

Fig 2. (a) XRD pattern and (b) N_2 adsorption-desorption isotherm of carbon aerogel

The porosity of the silica aerogel matrix material was determined by nitrogen adsorption/desorption porosimetry. The obtained isotherm shown in Fig. 2b can be classified as type IV, which is typical of mesoporous silica materials. The samples exhibit the presence of both macropores and mesopores (indicated by the sharply increasing adsorption isotherm above $P/P_0 = 0.9$ and the presence of the hysteresis. The BET surface area was 233.9 m^2/g, which is very high compared to similar studies [21].

The observed SEM images shown in Fig. 3a clearly reveal that cellulose aerogel is a combination of cellulose fiber exhibiting large channels with the average diameters in range of 10- 20 µm.

As mentioned above, the morphology of obtained carbon aerogels shown in Fig. 3b exhibit the porous structures and large channels with average diameter in range of 10 - 30 nm. It is also clear from the FESEM images that the channels are well connected with each other promising for the electrolyte ions diffusion. It is different from that before carbonization. Before carbonization, cellulose aerogels possess well-shaped mesoporous structures, with channels diameter are in range of 10 - 20 nm. Interestingly, the channels show the uniform diameter distribution, which is the typical characteristic of carbon aerogels.

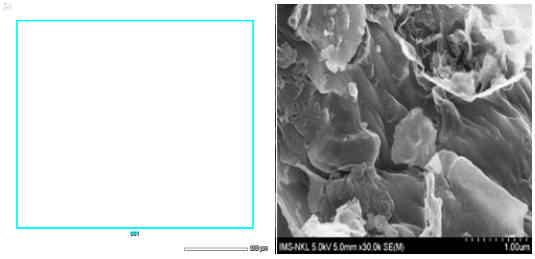

Fig 3. SEM images of (a) cellulose aerogel and (b) carbon aerogel

After carbonized, the uniform mesoporous structures of cellulose aerogel were broken and the mesopores left with very large crack. The transformation to such a porous structure of the pores was caused by the local melting of cellulose and carbonization of cellulose aerogel during heating and carbonization process. It is well known that the glass transition temperature of dried cellulose is around 200°C [22], and when the sample was heated to 200°C, the melting process of cellulose causes the connection ofcellulose molecules and form complete surface in some part of the aerogels due to the high surface tension. Because of the lack of enough mass of cellulose of the porous aerogels, the aerogels cannot connect to be an entire bulk structures, and the network is broken and forms porous structure [23]. The better understanding and visualization of carbon aerogel, EDX maps of carbon aerogel were shown in Fig.4, which present the element distribution of carbon and oxygen.

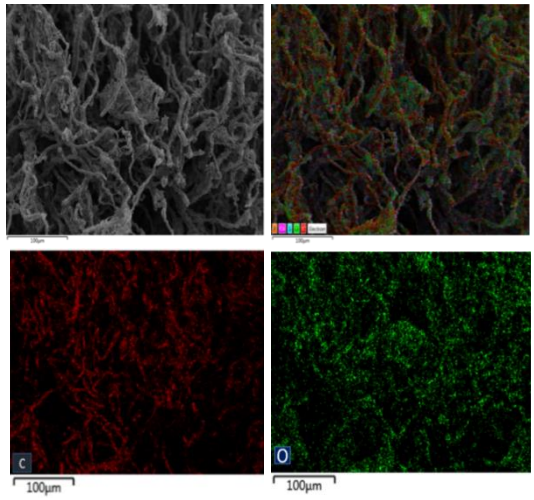

Fig.4 EDX mappi ng of carbon aerogel

Two electrodes of carbon aerogel - super P conductive - PVDF on nickel foil and an PP membrane were assembled to fabricate the symmetric supercapacitor. Cyclic Voltammetry curves of at different voltage range is shown in Fig.5.

Fig. 5a shows an almost rectangular shape of the voltammograms up to the highest voltage of 0.5 V thus evidencing the absence of parasitic undesired processes in the studied ranges of voltage window.

To evaluate the specific capacitance value with two-electrode configuration, galvanic charge-discharge tests were conducted (Fig. 5b) at various current densities. The charging curve is nearly symmetric with respect to the corresponding discharge curve in the potential range from 0 to 1.0 V.

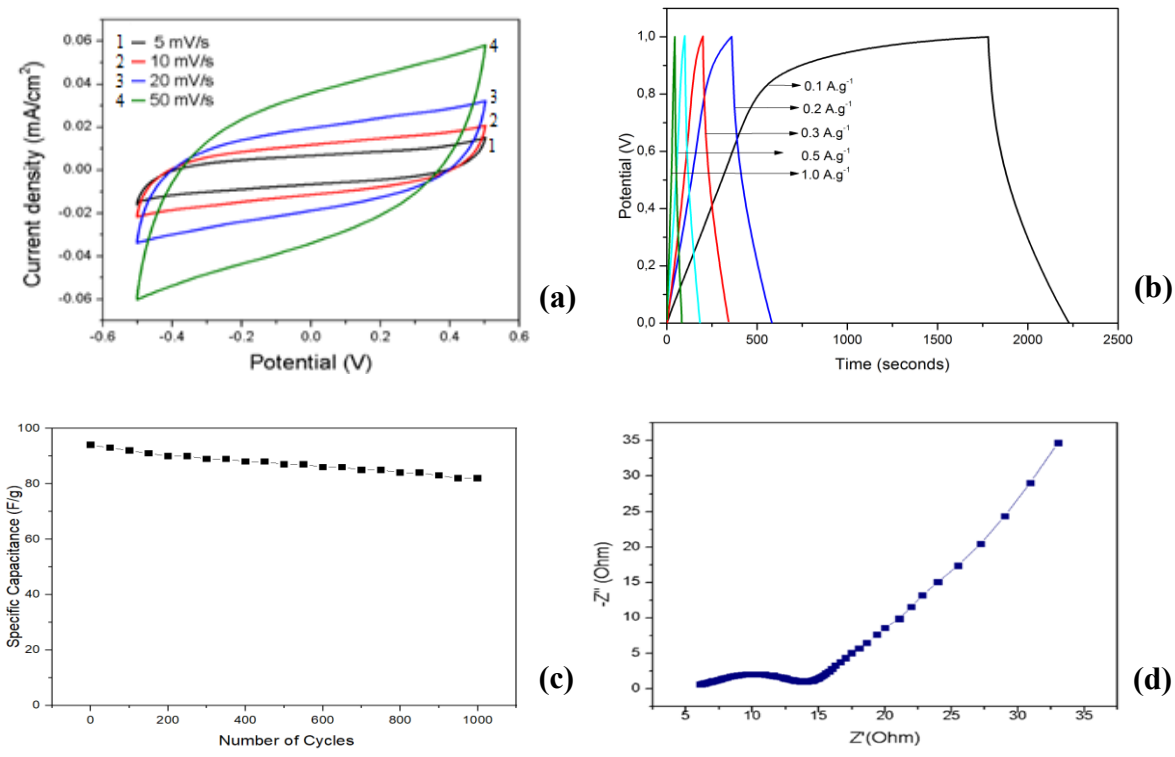

Fig 5. Electrochemical performance of carbon aerogel (a) CV curves, (b) GCD curves, (c) Nyquist plot and (d) long life

The specific capacitance of carbon aerogel electrode was calculated using the charge/discharge at current density of 0.1 to 1.0 A/g. The capacitance is high up to 94 F/g at 0.1 A/g and remains 80 F/g at 1.0 A/g.

Fig. 5c shows Nyquist plot of carbon aerogel electrode measured in 6 M KOH solution. Nyquist plot of electrode samples with starting point at Z'= 6.2 Ω representing the electrolyte resistance, and 8.4 Ω of diameter semi-circle indicating the charge transfer resistance. The 45° inclined line representing the Warburg impedance of the carbon aerogel electrode shows that the electrolyte ions can move easily through the mesopore of aerogel layer.

Subsequently, the long terms durability assessment of symmetric supercapacitor with two electrodes on copper foil was carried out. The SC is subjected to GCD sequences. This test procedure was repeated with sets of 1000 cycles. In this way, the performance of SCs is followed under stringent test conditions. The Fig. 5d shows that the capacitance of supercapacitor based on carbon aerogel remains 92.5% after 1000 cycles.

4. CONCLUSION

Carbon aerogel was successfully prepared from waste paper. The characterization and electrochemical performance of aerogel material were studied. The obtained carbon aerogel shows high specific surface area of 233.9 m^2/g. In a symmetric two electrode capacitor system, the carbon aerogel electrode exhibited a high specific capacitance of 94 F/g and a high cycle stability with a capacitance retention of 92.5% after 1000 cycles. This study could provide a novel route for high-performance energy storage materials derived from biomass waste.

Acknowledgement:

This research is funded by Science and Technology Development Project (number:788/2021).

REFERENCES

[1] 1.An, H., Y. Wang, X. Wang, L. Zheng, X. Wang, L. Yi, L. Bai, and X. Zhang, (2010). Polypyrrole/carbon aerogel composite materials for supercapacitor. *Journal of Power Sources*, **195(19)**, 6964-6969.

[2] Zhuo, H., Y. Hu, Z. Chen and L. Zhong, (2019). Cellulose carbon aerogel/PPy composites for high-performance supercapacitor. *Carbohydrate Polymers*, **215**, 322-329.

[3] Chen, G.-F., X.-X. Li, L.-Y. Zhang, N. Li, T.Y. Ma and Z.-Q. Liu, (2016). A Porous Perchlorate-Doped Polypyrrole Nanocoating on Nickel Nanotube Arrays for Stable Wide-Potential-Window Supercapacitors. *Advanced Materials*, **28(35)**, 7680-7687.

[4] Li, J., X. Yuan, C. Lin, Y. Yang, L. Xu, X. Du, J. Xie, J. Lin, and J. Sun, (2017). Achieving High Pseudocapacitance of 2D Titanium Carbide (MXene) by Cation Intercalation and Surface Modification. *Advanced Energy Materials*, **7(15)**, 1602725.

[5] Liu, Z.-Q., G.-F. Chen, P.-L. Zhou, N. Li and Y.-Z. Su, (2016). Building layered NixCo2x(OH)6x nanosheets decorated three-dimensional Ni frameworks for electrochemical applications. *Journal of Power Sources*, **317**, 1-9.

[6] Pan, Y., H. Gao, M. Zhang, L. Li and Z. Wang, (2017). Facile synthesis of ZnCo2O4 micro-flowers and micro-sheets on Ni foam for pseudocapacitor electrodes. *Journal of Alloys and Compounds*, **702**, 381-387.

[7] Chen, X.Y., C. Chen, Z.J. Zhang and D.H. Xie, (2013). High performance porous carbon through hard–soft dual templates for supercapacitor electrodes. *Journal of Materials Chemistry A*, **1(25)**, 7379-7383.

[8] El-Kady, M., V. Strong, S. Dubin and R. Kaner, (2012). Laser Scribing of High-Performance and Flexible Graphene-Based Electrochemical Capacitors. *Science (New York, N.Y.)*, **335(6074)**, 1326-1330.

[9] Miller, J.R. and P. Simon, (2008). Electrochemical capacitors for energy management. *Science Magazine*, **321(5889)**, 651-652.

[10] Simon, P. and Y. Gogotsi, (2008). Materials for electrochemical capacitors. *Nature Materials*, **7(11)**, 845-854.

[11] Yu, G., X. Xie, L. Pan, Z. Bao and Y. Cui, (2013). Hybrid nanostructured materials for high-performance electrochemical capacitors. *Nano Energy*, **2(2)**, 213-234.

[12] Bose, S., T. Kuila, A.K. Mishra, R. Rajasekar, N.H. Kim and J.H. Lee, (2012). Carbon-based nanostructured materials and their composites as supercapacitor electrodes. *Journal of Materials Chemistry*, **22(3)**, 767-784.

[13] Li, X.-X., G.-F. Chen, K. Xiao, N. Li, T.-Y. Ma and Z.-Q. Liu, (2017). Self-supported amorphous-edge nickel sulfide nanobrush for excellent energy storage. *Electrochimica Acta*, **255**, 153-159.

[14] Wang, X., S. Kajiyama, H. Iinuma, E. Hosono, S. Oro, I. Moriguchi, M. Okubo, and A. Yamada, (2015). Pseudocapacitance of MXene nanosheets for high-power sodium-ion hybrid capacitors. *Nature communications*, **6(1)**, 1-6.

[15] Niu, Z., H. Dong, B. Zhu, J. Li, H.H. Hng, W. Zhou, X. Chen, and S. Xie, (2013). Highly stretchable, integrated supercapacitors based on single-walled carbon nanotube films with continuous reticulate architecture. *Advanced Materials*, **25(7)**, 1058-1064.

[16] Le, T.H., V.H. Ngo, M.T. Nguyen, V.C. Nguyen, D.N. Vu, T.D. Pham, and D.T. Tran, (2021). Enhanced Electrochemical Performance of Porous Carbon Derived from Cornstalks for Supercapacitor Applications. *Journal of Electronic Materials*, **50(12)**, 6854-6861.

[17] Si, W., J. Zhou, S. Zhang, S. Li, W. Xing and S. Zhuo, (2013). Tunable N-doped or dual N, S-doped activated hydrothermal carbons derived from human hair and glucose for supercapacitor applications. *Electrochimica acta*, **107**, 397-405.

[18] Sun, H., L. Cao and L. Lu, (2012). Bacteria promoted hierarchical carbon materials for high-performance supercapacitor. *Energy & Environmental Science*, **5(3)**, 6206-6213.

[19] Zhu, Y., S. Murali, M.D. Stoller, K. Ganesh, W. Cai, P.J. Ferreira, A. Pirkle, R.M. Wallace, K.A. Cychosz, and M. Thommes, (2011). Carbon-based supercapacitors produced by activation of graphene. *science*, **332(6037)**, 1537-1541.

[20] Zhi, M., C. Xiang, J. Li, M. Li and N. Wu, (2013). Nanostructured carbon–metal oxide composite electrodes for supercapacitors: a review. *Nanoscale*, **5(1)**, 72-88.

[21] Bi, H., X. Huang, X. Wu, X. Cao, C. Tan, Z. Yin, X. Lu, L. Sun, and H. Zhang, (2014). Carbon Microbelt Aerogel Prepared by Waste Paper: An Efficient and Recyclable Sorbent for Oils and Organic Solvents. *Small (Weinheim an der Bergstrasse, Germany)*, **10**(17), 3544-3550.

[22] Szcześniak, L., A. Rachocki and J. Tritt-Goc, (2008). Glass transition temperature and thermal decomposition of cellulose powder. *Cellulose*, **15(3)**, 445-451.

[23] Hao, P., Z. Zhao, J. Tian, H. Li, Y. Sang, G. Yu, H. Cai, H. Liu, C. Wong, and A. Umar, (2014). Hierarchical porous carbon aerogel derived from bagasse for high performance supercapacitor electrode. *Nanoscale*, **6(20)**, 12120-12129.